

# SCIENTIFIC REPORTS



OPEN

## Sulfation of the FLAG epitope is affected by co-expression of G protein-coupled receptors in a mammalian cell model

Morag Rose Hunter<sup>†</sup>, Natasha Lillia Grimsey & Michelle Glass

Received: 03 March 2016

Accepted: 15 May 2016

Published: 07 June 2016

G protein-coupled receptors (GPCRs) are important therapeutic targets and therefore extensively studied. Like most transmembrane proteins, there has been considerable difficulty in developing reliable specific antibodies for them. To overcome this, epitope tags are often used to facilitate antibody recognition in studies on fundamental receptor signalling and trafficking. In our study of cannabinoid CB<sub>1</sub>/dopamine D<sub>2</sub> interactions we sought to generate HEK293 cells expressing FLAG-tagged D<sub>2</sub> for use in antibody-based assays of GPCR localisation and trafficking activity, however observed that stable FLAG-hD<sub>2</sub> expression was particularly challenging to maintain. In contrast, when expressed in cell lines expressing hCB<sub>1</sub> robust and stable FLAG-hD<sub>2</sub> expression was observed. We hypothesised that co-expression of CB<sub>1</sub> might stabilise surface FLAG-hD<sub>2</sub> expression, and therefore investigated this further. Here, we describe the observation that co-expression of either cannabinoid CB<sub>1</sub> or CB<sub>2</sub> receptors in HEK293 decreases the sulfation of a FLAG epitope appended at the N-terminus of the dopamine D<sub>2</sub> receptor. Sulfation alters epitope recognition by some anti-FLAG antibodies, leading to the detection of fewer receptors, even though expression is maintained. This demonstrates that cannabinoid receptor expression modifies posttranslational processing of the FLAG-hD<sub>2</sub> receptor, and importantly, has wider implications for the utilisation and interpretation of receptor studies involving epitope tags.

G protein-coupled receptors (GPCRs) are a large family of proteins which are found embedded into cellular membranes, typically on the cell surface. The general structure of GPCRs is well conserved, with an extracellular N-terminal tail, seven transmembrane alpha-helices joined by intra- and extra-cellular loops, an intracellular eighth helix, and an intracellular C-terminal tail<sup>1</sup>. As their name suggests, GPCRs activate G proteins by acting as a cofactor for the exchange of GDP to GTP on the G $\alpha$  subunit<sup>2</sup>.

GPCRs are able to function both as monomers, and in groups of two (dimers) or more (oligomers). Dimers and higher order oligomers may be composed of several different GPCRs (heterodimers, or “mosaics”)<sup>3,4</sup>. For most Class A GPCRs, it is unknown whether dimerisation is required for normal function. However, there is extensive description of heterodimer formation and function in mammalian cell systems (reviewed in<sup>5,6</sup>). Generally, GPCR heterodimers have a more restricted tissue distribution than their component receptors. Thus, therapeutics focusing on heterodimers may offer the opportunity to selectively target a specific subset of receptors within the body and exploit dimer-specific signalling pathways.

One such heterodimer consists of the cannabinoid receptor 1 (CB<sub>1</sub>) and dopamine receptor 2 (D<sub>2</sub>). There is considerable behavioural evidence that the cannabinoid and dopamine systems interact in the rodent and human brain, affecting motor functioning and the reward pathway<sup>7</sup>. CB<sub>1</sub> and D<sub>2</sub> are co-localised in GABAergic synapses in the prefrontal cortex<sup>8</sup> and the nucleus accumbens<sup>9</sup>.

Although both CB<sub>1</sub> and D<sub>2</sub> canonically signal through G $\alpha$ i pathways, this changes to an apparently G $\alpha$ s signalling pathway when the receptors are co-stimulated in medium spiny neurons, which endogenously express both CB<sub>1</sub> and D<sub>2</sub><sup>10</sup>. This signalling switch could be replicated in Human Embryonic Kidney cells (HEK293)<sup>11</sup>, and has been found to be dependent on the co-expression of these two receptors<sup>12</sup>, leading to the hypothesis that this was due to a direct physical interaction between the two receptors - i.e. heterodimerisation. Results consistent

Department of Pharmacology and Clinical Pharmacology, University of Auckland, Auckland, New Zealand. <sup>†</sup>Present address: Department of Pathology, University of Cambridge, Cambridge, United Kingdom. Correspondence and requests for materials should be addressed to M.G. (email: m.glass@auckland.ac.nz)

with heterodimerisation have been demonstrated by co-immunoprecipitation experiments<sup>11,13</sup>, fluorescence resonance energy transfer<sup>14–16</sup> and bimolecular fluorescence complementation<sup>17</sup>. Furthermore, in medium spiny neurons, knockdown of either CB<sub>1</sub> or D<sub>2</sub> receptors reduced the expression of the other<sup>18</sup>, suggesting that protein levels are closely controlled by the activity of both receptors.

In our study of CB<sub>1</sub>/D<sub>2</sub> interactions we sought to generate HEK293 cell lines expressing FLAG-tagged human (h) D<sub>2</sub> for use in antibody-based assays of GPCR localisation and trafficking activity, however we observed that stable FLAG-hD<sub>2</sub> expression was particularly challenging to maintain. When introduced alone, the long-term maintenance of a HEK293 cell line with measurable FLAG-hD<sub>2</sub> expression proved apparently impossible. While we could transiently express the FLAG-hD<sub>2</sub> construct easily in HEK293 wildtype cells, expression (as measured by antibody labelling) was very low immediately following antibiotic selection. However, we were interested to note that HEK293 cell lines which also expressed introduced hCB<sub>1</sub> (with a triple HA tag “3HA”) exhibited robust FLAG-hD<sub>2</sub> expression and stable lines were established with relative ease. We hypothesised that co-expression of the 3HA-hCB<sub>1</sub> receptor might stabilise surface FLAG-hD<sub>2</sub> expression, and therefore investigated this further.

## Results

**Antibody detection of FLAG-hD<sub>2</sub> throughout the establishment of stable cell lines.** In order to investigate whether FLAG-hD<sub>2</sub> expression was facilitated by co-expression of hCB<sub>1</sub>, HEK293 cell lines (hereafter “HEK”) were transfected with the FLAG-hD<sub>2</sub> pcDNA3.1+ plasmid and subjected to antibiotic selection to generate stable cell lines. The parental cell lines into which FLAG-hD<sub>2</sub> was transfected were HEK wildtype (wt), or HEK stably transfected with either 3HA-hCB<sub>1</sub> or 3HA-hCB<sub>2</sub>. A subset of transfected cells were also cultured without antibiotic selection. Antibody labelling was measured every second passage for 56 days in order to monitor FLAG-hD<sub>2</sub> expression over time. A clonally-isolated positive control cell line, already characterised in our laboratory as expressing both 3HA-hCB<sub>1</sub> and FLAG-hD<sub>2</sub> (i.e., the expected result of the HEK 3HA-hCB<sub>1</sub>+FLAG-hD<sub>2</sub> transfection condition), was used as a labelling control, as this had already been demonstrated to exhibit anti-FLAG antibody labelling.

Utilising a mouse monoclonal anti-FLAG antibody, striking differences in the apparent proportion of cells expressing surface FLAG-hD<sub>2</sub> were observed depending on the cell background utilised. Following transfection into HEK wt, transient FLAG-hD<sub>2</sub> expression was detected during the first 10 days of culture, however the proportion of FLAG-hD<sub>2</sub> positive cells subsequently decreased during antibiotic selection (which took approximately 14–18 days, as determined by the death of all cells in a flask of untransfected cells), after which FLAG labelling was nearly completely lost (Fig. 1a,f,g). Conversely, when transfected into a previously established HEK 3HA-hCB<sub>1</sub> line<sup>19</sup> detection of FLAG-hD<sub>2</sub> was retained during the selection phase, and the proportion of expressing cells tended to increase with continued selection pressure, as is typically expected on the establishment of a cell line stably expressing the introduced gene of interest (Fig. 1c,f,g). A similar pattern was observed when FLAG-hD<sub>2</sub> was transfected into a 3HA-hCB<sub>2</sub>-expressing HEK cell line, where the ability to detect FLAG-hD<sub>2</sub> was retained with long term culture (Fig. 1e–g). We also noted that only approximately 80% of the positive-control HEK FLAG-hD<sub>2</sub>/3HA-hCB<sub>1</sub> cell line was indicated to express FLAG-hD<sub>2</sub>, even though this line was derived by clonal isolation.

To validate these findings, and to permit co-labelling with mouse anti-HA antibody to detect 3HA-hCB<sub>1</sub>, we performed parallel immunocytochemistry experiments on the same cells as assayed above with a polyclonal rabbit anti-FLAG antibody. Surprisingly, labelling with this antibody indicated approximately equivalent proportions of FLAG-positive cells between the HEK wt, 3HA-hCB<sub>1</sub> and 3HA-hCB<sub>2</sub> cell backgrounds (Fig. 1b,d,e–g). After long-term culture (day 56, 16 passages post-transfection) the proportion of cells labelled with rabbit anti-FLAG remained approximately unchanged when compared to day 21, regardless of the parental cell line (comparison of rabbit anti-FLAG labelling on day 21 versus day 56 in HEK wt, HEK 3HA-hCB<sub>1</sub>, and HEK 3HA-hCB<sub>2</sub>;  $p > 0.05$ ), although overall more cells were labelled with rabbit anti-FLAG antibody when the cell background contained 3HA-hCB<sub>1</sub> or 3HA-hCB<sub>2</sub>, as compared with HEK wt cells ( $85 \pm 3\%$ ,  $93 \pm 4\%$  and  $66 \pm 7\%$ , respectively; Fig. 1b,d–g). This antibody indicated that close to 100% of the positive-control HEK FLAG-hD<sub>2</sub>/3HA-hCB<sub>1</sub> cells expressed FLAG-hD<sub>2</sub>, as was expected due to the clonal nature of this line.

Importantly, under the conditions utilised in these experiments neither anti-FLAG antibody labelled the untransfected parental cell lines, indicating a lack of non-specific binding (Fig. 1a–d).

The intensity of antibody labelling was also compared across the transfection conditions. Using the same microscopy images as were analysed to measure the proportion of positively stained cells, the total intensity of antibody labelling above background was averaged across all cells in the image. Since each anti-FLAG antibody provides a different absolute level of staining, labelling was normalised so that untransfected HEK wt cells were set to 0%, and the HEK 3HA-hCB<sub>1</sub>/FLAG-hD<sub>2</sub> control line was set to 100% labelling for each anti-FLAG antibody.

The intensity analysis demonstrated differences in the degree of anti-FLAG labelling between the parental cell lines, but overall was in agreement with the prior measured proportions of positive cells. On day 2, in the transient transfection phase, there was low average FLAG-hD<sub>2</sub> labelling (Fig. 1h). This is likely a reflection of the small proportion of cells which were initially transfected. By day 21, at the conclusion of antibiotic selection, the transfected HEK wt cell was essentially devoid of mouse anti-FLAG labelling, whereas a moderate degree of FLAG-hD<sub>2</sub> labelling was detected in the 3HA-hCB<sub>1</sub> line with this antibody (Fig. 1i). By comparison, the rabbit anti-FLAG antibody produced significantly more labelling than the mouse antibody. Though the indicated labelling per cell was considerably lesser than that of the positive control line, this was likely a result of these lines being mixed populations comprised of cells with a range of expression levels as opposed to the clonal HEK 3HA-hCB<sub>1</sub>/FLAG-hD<sub>2</sub> control. Interestingly, FLAG-hD<sub>2</sub> labelling by both antibodies was considerably higher in the HEK 3HA-hCB<sub>2</sub> cell background than in the HEK 3HA-hCB<sub>1</sub> background.

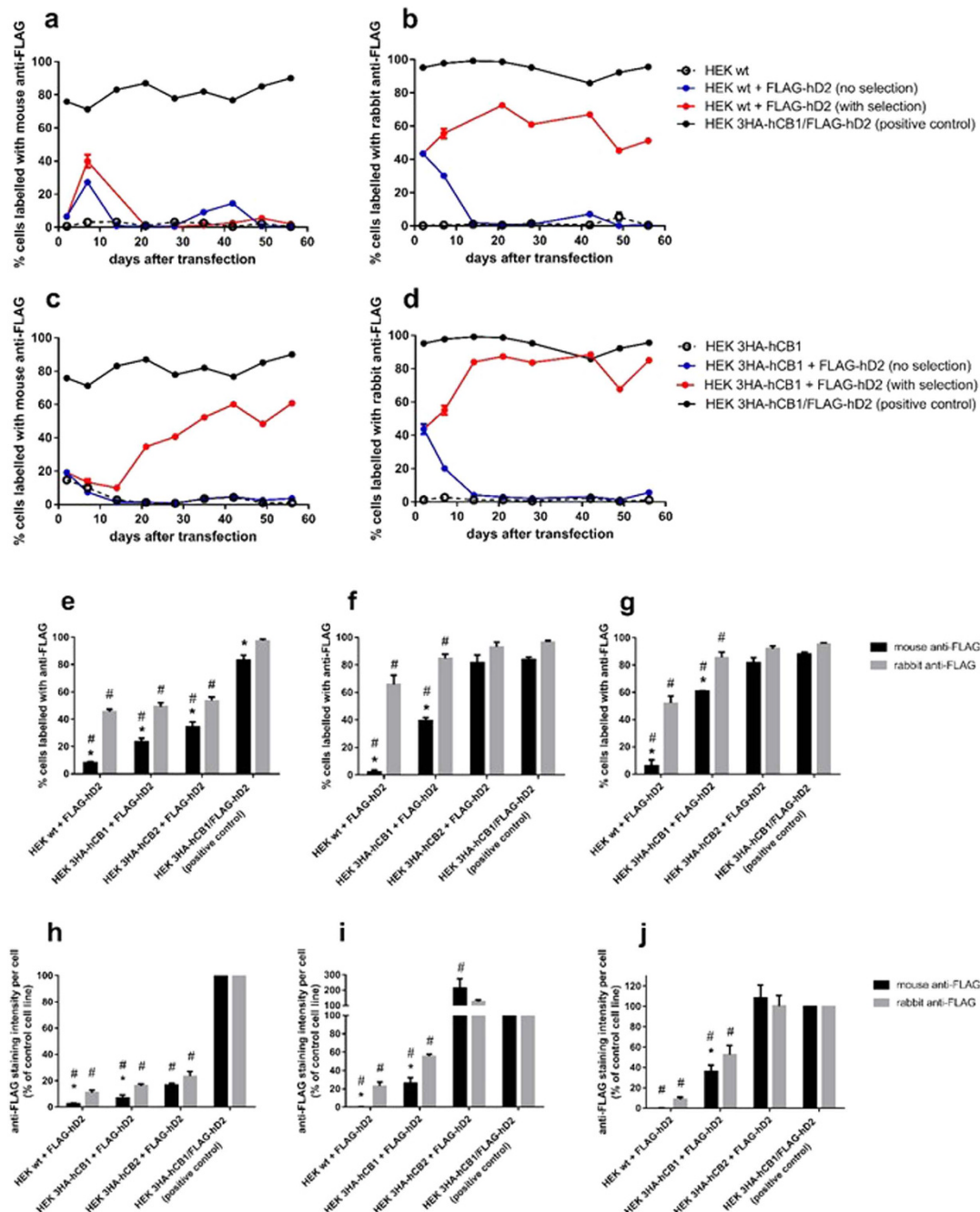


**Figure 1. Immunocytochemical analysis of cells exhibiting cell surface FLAG-hD<sub>2</sub> labelling following transfection into different HEK cell backgrounds, as detected by two anti-FLAG antibodies; time course post-transfection.** FLAG-hD<sub>2</sub> was transfected into HEK wt (a,b,e,h), HEK 3HA-hCB<sub>1</sub> (c,d,f,i), or HEK 3HA-hCB<sub>2</sub> (g,j) cell backgrounds. Surface receptors were stained with either mouse anti-FLAG M2 monoclonal (a,c), or rabbit anti-FLAG polyclonal (b,d) antibodies for 56 days after transfection, with specific analysis at 2 days (transient expression phase; e,h), 21 days (immediately after stable selection; f,i), and 56 days (after continuous maintenance in selection antibiotic; g,j). Images were taken by automated microscopy at 10x magnification and the resultant images were analysed for the proportion of cells positive for anti-FLAG labelling (a–g), and the labelling intensity (g–j) were analysed. Representative data (one of three independent experiments) showing the time-course of anti-FLAG labelling intensity for the experimental samples (red) compared to that of the untransfected parental cell line (dashed lines), cells transfected but not subjected to antibiotic selection pressure (blue), and a clonal control cell line stably expressing 3HA-hCB<sub>1</sub> and FLAG-hD<sub>2</sub> (black) (A–D). Combined data (mean + SEM) from three independent experiments comparing anti-FLAG labelling patterns at key time points (e–j). Intensity analysis is normalised to matched labelling of untransfected HEK wt cells (0%) and the HEK 3HA-hCB<sub>1</sub>/FLAG-hD<sub>2</sub> control cell line (100%) (h–j).  $p < 0.05$ , \*significant difference within cell line labelled with rabbit anti-FLAG versus mouse anti-FLAG; #significant difference compared to HEK 3HA-hCB<sub>1</sub>/FLAG-hD<sub>2</sub> control cell line with same antibody.

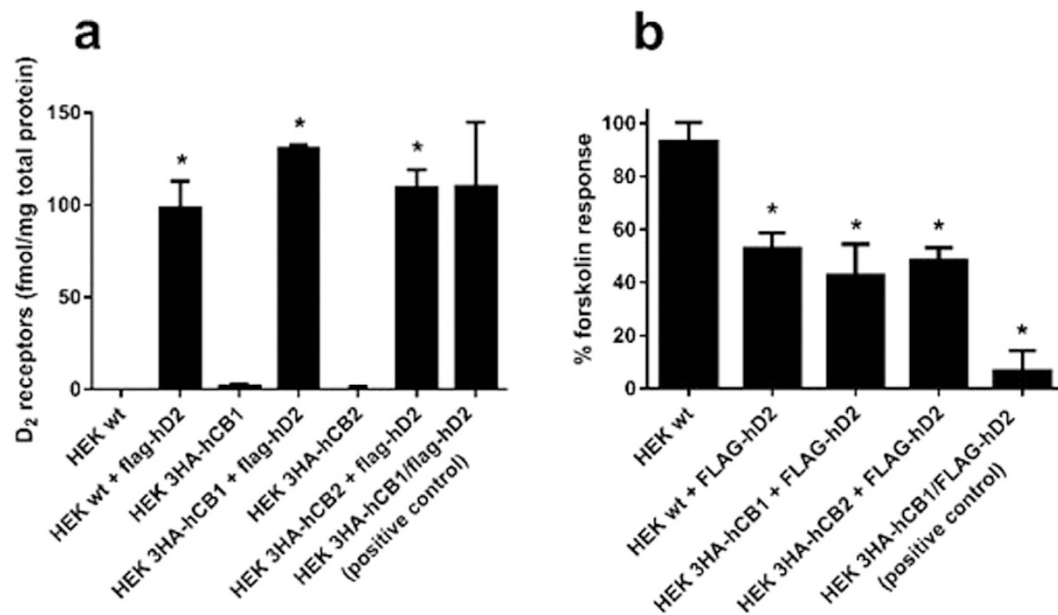


**Figure 2.** [<sup>3</sup>H]-raclopride whole-cell binding and cAMP signalling in HEK cell lines stably transfected with FLAG-D<sub>2</sub>. Cells were stably transfected with FLAG-hD<sub>2</sub> and assayed day 56–57/16 passages post-transfection. [<sup>3</sup>H]-raclopride binding assays were performed, demonstrating approximately equal numbers of D<sub>2</sub> binding sites between all FLAG-hD<sub>2</sub>-transfected cell lines, but not in untransfected cell lines (a). Mean ± SEM of three independent experiments, \*p < 0.05 significant compared to untransfected parental cell line. The ability of 100 nM quinpirole to inhibit 5 μM forskolin-induced cAMP increase was measured using a cAMP biosensor over 15 minutes of stimulation in cell lines 57 days/16 passages post-transfection with FLAG-hD<sub>2</sub> (other than “HEK wt” which was not transfected) (b). cAMP responses were normalised to forskolin alone (100%) and vehicle (0%). Mean + SEM of three independent experiments. p < 0.05; \*significant inhibition compared to forskolin alone.

Due to the markedly different labelling observed with the rabbit anti-FLAG and mouse anti-FLAG antibodies, binding and functional studies were carried out as alternative means to determine FLAG-hD<sub>2</sub> expression in the cell lines generated.

**Determination of D<sub>2</sub> expression by radioligand binding.** To determine receptor number, whole cell radioligand binding assays were performed 56–57 days (16 passages) post-transfection with [<sup>3</sup>H]-raclopride, a D<sub>2</sub>-selective antagonist. All cells transfected and selected for FLAG-hD<sub>2</sub> expression contained approximately equivalent receptor levels of 98–131 fmol D<sub>2</sub> receptors per mg of total cell protein (no statistically significant differences; Fig. 2a). Negligible specific binding was detected the cell lines not transfected with hD<sub>2</sub>, indicating that it was the introduced FLAG-hD<sub>2</sub> transgene which conferred [<sup>3</sup>H]-raclopride binding in these samples.

**Demonstration of FLAG-hD<sub>2</sub> functionality by cAMP signalling assay.** To determine receptor functionality, cAMP assays were performed 57 days/16 passages post-transfection with quinpirole, a D<sub>2</sub>-selective agonist. As shown in Fig. 2b, all transfected cells were responsive to quinpirole (100 nM) as indicated by a reduction in cAMP relative to forskolin alone (100%) and as expected for a G<sub>o</sub>i-coupled receptor. FLAG-hD<sub>2</sub>-transfected cell lines which had originally contained 3HA-hCB<sub>1</sub> or 3HA-hCB<sub>2</sub> retained their responsiveness to CP55,940, a non-selective CB<sub>1</sub>/CB<sub>2</sub> agonist (data not shown). All three experimental cell lines trended towards less responsiveness to quinpirole as compared to the HEK 3HA-hCB<sub>1</sub>/FLAG-hD<sub>2</sub> positive control cell line. Though this difference was not statistically significant, this apparent lesser responsiveness was not unexpected given that the experimental cell lines were mixed populations with a range of receptor levels, compared to the clonal, high expressing HEK 3HA-hCB<sub>1</sub>/FLAG-hD<sub>2</sub> cell line. However, the newly-generated FLAG-hD<sub>2</sub>-transfected cell lines exhibited an equivalent degree of D<sub>2</sub>-mediated signalling, regardless of whether hCB<sub>1</sub>, hCB<sub>2</sub> or neither were expressed when hD<sub>2</sub> was introduced.

**Determination that antibody recognition is sensitive to sulfation.** Having observed a stark contrast between the results of antibody labelling experiments (which suggested highly variable FLAG-hD<sub>2</sub> expression between transfection conditions) and the radioligand binding and cAMP results (which indicated similar D<sub>2</sub> expression in all transfection conditions), we hypothesised that the FLAG antibodies were differentially sensitive to a feature of the FLAG epitope which was present when D<sub>2</sub> was expressed alone, but not when expressed with CB<sub>1</sub> or CB<sub>2</sub>. The tyrosine residue in FLAG has previously been reported as being sulfated<sup>20,21</sup>, therefore we treated cells with sodium chlorate to inhibit sulfation<sup>22</sup>. Treated and untreated cells were then stained for cell surface FLAG epitope, and imaged by automated microscopy as above.

Vastly greater anti-FLAG labelling intensity was found in cells treated with sodium chlorate (Fig. 3). We verified that this treatment did not affect the nonspecific labelling of either antibody on untransfected cells. Qualitatively, these images demonstrate that anti-FLAG labelling (with both the mouse and rabbit antibodies) was increased in all FLAG-expressing cell lines when sulfation was inhibited using sodium chlorate. Importantly, following sodium chlorate treatment, both FLAG antibodies now indicate essentially equivalent FLAG-hD<sub>2</sub> expression regardless of the cell background into which they were transfected. As well as now reflecting a consistent antibody labelling pattern between the two antibodies, this finding aligned with our radioligand binding and cAMP functional data that likewise indicated similar expression levels.

## Discussion

Epitope tags are commonly used for experiments requiring immunocytochemical detection of exogenous GPCRs, primarily because antibodies are difficult to raise to endogenous GPCR epitopes<sup>23–26</sup> and also to reduce reagent costs. The commercially-available antibodies to epitope tags such as haemagglutinin (“HA”) and DYKXXD (“FLAG”) are well established in the literature, making the use of epitope tags an attractive approach to experiments which would otherwise require the generation and validation of GPCR-specific antibodies.

The hD<sub>2</sub> construct utilised in this study is N-terminally FLAG-tagged, and indeed “FLAG” has been specifically recommended for receptor internalisation assays<sup>27,28</sup>. Anti-FLAG antibodies were employed to label this FLAG-hD<sub>2</sub> transgene with the aim of measuring relative protein expression. We were interested to observe that co-expression of either 3HA-hCB<sub>1</sub> or 3HA-hCB<sub>2</sub> influenced the degree of FLAG-hD<sub>2</sub> labelling; seemingly indicating that co-expression with cannabinoid receptors may increase hD<sub>2</sub> surface expression. This finding was re-capitulated with two different FLAG antibodies, though to differing extents.

The two commercially-available anti-FLAG antibodies we compared were polyclonal rabbit anti-FLAG (Sigma, cat. F7425) and monoclonal mouse anti-FLAG M2 (Sigma, cat. F1804). While there was negligible non-specific binding to untransfected cells, an important difference was seen between the ability of the antibodies to detect the FLAG epitope. The mouse anti-FLAG antibody essentially indicated a complete lack of FLAG-hD<sub>2</sub> expression, *unless* the transgene was introduced into cells already expressing either 3HA-hCB<sub>1</sub> or 3HA-hCB<sub>2</sub>. Although the rabbit anti-FLAG antibody could detect FLAG-hD<sub>2</sub> transfected into the HEK wt line, labelling intensity was again greater in the 3HA-hCB<sub>1</sub> and 3HA-hCB<sub>2</sub> lines.

This interesting finding of an apparent cannabinoid receptor-induced alteration of hD<sub>2</sub> expression was, however, called into question by our follow-up experiments examining D<sub>2</sub>-selective radioligand binding and cAMP signalling. These instead indicated that hD<sub>2</sub> expression was equivalent between the cell backgrounds tested, irrespective of the presence of 3HA-hCB<sub>1</sub> or 3HA-hCB<sub>2</sub>. Given these measures are a more direct indication of D<sub>2</sub> expression and functionality than anti-FLAG labelling (and that a prior report had also suggested that D<sub>2</sub> ligand binding is unaffected by CB<sub>1</sub> co-expression<sup>11</sup>), we hypothesised that the fidelity of the anti-FLAG labelling was questionable.

Some antibodies are known to be sensitive to epitope post-translational modifications, including the M2 mouse monoclonal antibody used in this study, which has been reported to be sensitive to sulfation<sup>20,21</sup>. Tyrosine sulfation occurs in the Golgi<sup>29</sup>, and is a common posttranslational modification of secreted and transmembrane proteins (reviewed in<sup>30</sup>). Tyrosine sulfation is more likely when the tyrosine residue is surrounded by acidic residues (summarised in<sup>31</sup>), making the FLAG epitope a likely target, as it contains one aspartic acid in the -1 position, and four aspartic acid residues in positions +2 to +5, relative to the tyrosine. Furthermore, the lysine in the +1 position is also consistent with a tyrosine sulfation site, as nearby polar residues are more permissive of this modification<sup>31</sup>. Sulfation of the FLAG epitope has been shown to prevent the mouse anti-FLAG M2 antibody from binding and reduces the binding of other anti-FLAG antibodies<sup>21,22</sup>. Indeed, sulfation of the N-terminus has been observed for several GPCRs, including the sphingosine 1-phosphate S1P1 receptor<sup>32</sup>, chemokine CCR2 receptor<sup>22</sup>, and complement component 5a C5aR1 receptor<sup>33</sup>. These previously-reported observations led us to test whether sulfation was a factor in antibody binding in our experimental system.

Cells were treated with sodium chlorate to reduce sulfation activity<sup>22,34–36</sup>, resulting in a considerable increase in labelling of both the mouse M2 monoclonal and rabbit polyclonal anti-FLAG antibodies. This is consistent with unmasking of the FLAG epitope by removal of sulfation. These results indicate that the predominant idiotypes in the polyclonal rabbit anti-FLAG are also unable to detect sulfated FLAG-hD<sub>2</sub>, thereby giving inconsistent and potentially misleading results when comparing cell lines or drug treatments where sulfation is occurring differently.

When we look specifically at D<sub>2</sub>, the addition of the FLAG epitope on the D<sub>2</sub> N-terminus is a relatively common way of monitoring D<sub>2</sub> receptor expression and trafficking (for example<sup>11,37,38–40</sup>), usually without a second antibody to compare labelling profiles. Additionally, the mouse M2 anti-FLAG antibody specifically has been used for detection of N-terminally-tagged FLAG-hD<sub>2</sub><sup>38–41</sup>, which this study has shown has a high sensitivity to the sulfation state of the FLAG-hD<sub>2</sub> construct. In light of the results of this study, future work should be designed to avoid or account for this phenomenon.

The results of our stable transfection experiments showed that expression of 3HA-hCB<sub>1</sub> or 3HA-hCB<sub>2</sub> modifies the detectability of the FLAG-hD<sub>2</sub> transgene. CB<sub>1</sub> and D<sub>2</sub> receptors are known to form a heterodimer, with many of these studies carried out in HEK293 cells<sup>11,13–15,17</sup>. It is possible that a physical interaction of CB<sub>1</sub> and D<sub>2</sub> while trafficking via the synthetic pathway protects the FLAG epitope in the FLAG-hD<sub>2</sub> construct from sulfation, perhaps either by altering the conformation of the D<sub>2</sub> N-terminal tail or by otherwise altering sulfotransferases' access to the FLAG epitope. When designing these experiments, CB<sub>2</sub> was chosen as a control cell line because we know of no published evidence suggesting that a CB<sub>2</sub>-D<sub>2</sub> heterodimer exists. Therefore, it was a surprise to find that 3HA-hCB<sub>2</sub> expression also altered FLAG-hD<sub>2</sub> posttranslational modification. Although there are no reported studies describing CB<sub>2</sub>-D<sub>2</sub> heterodimeric or signalling interactions, GPCRs can form non-physiologically relevant heterodimers in transfected cell lines (for example the dopamine D<sub>1</sub>-D<sub>2</sub> heterodimer, which appears to have a

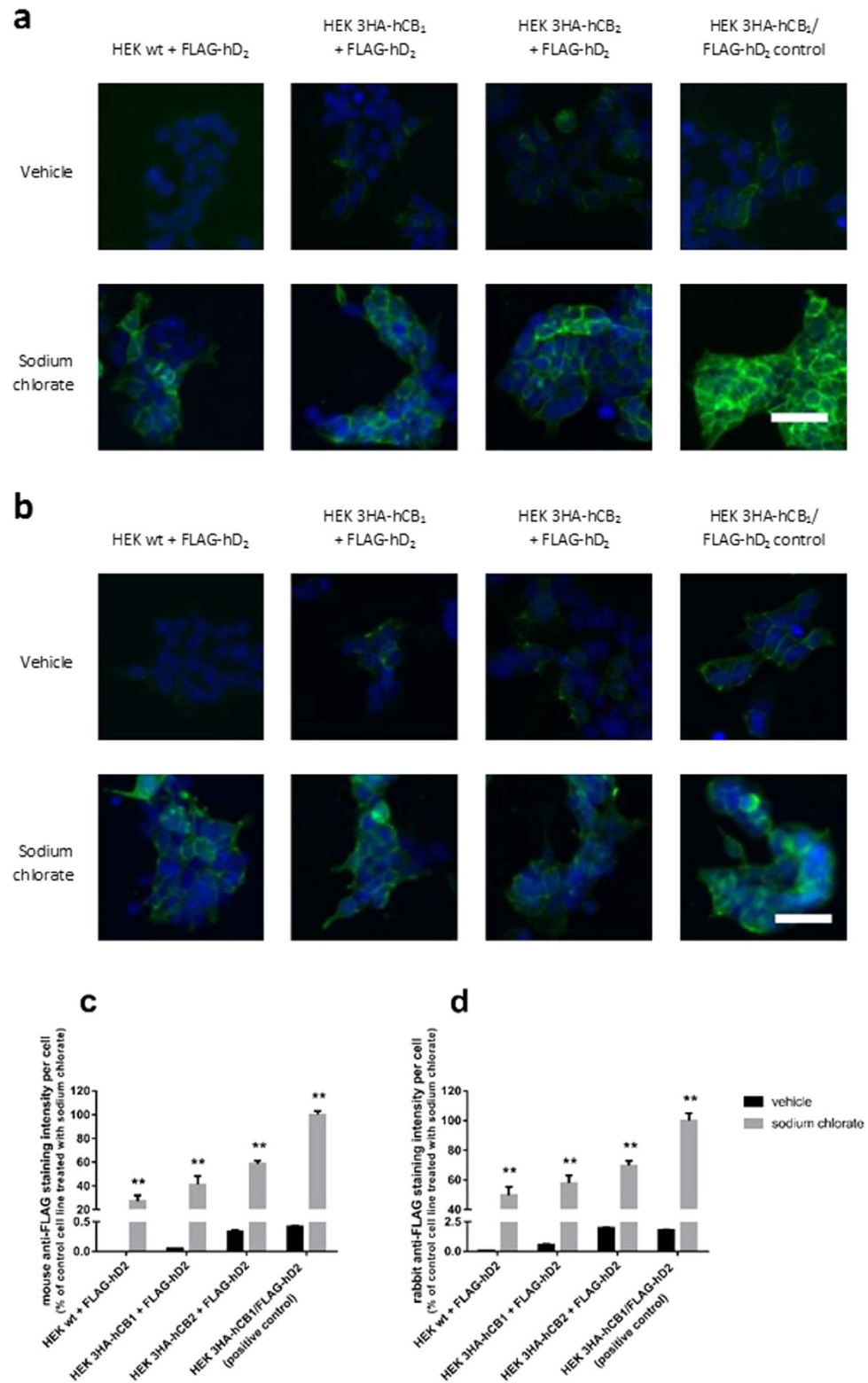


**Figure 3. Antibody labelling with two anti-FLAG antibodies with and without inhibition of sulfation with sodium chlorate.** Cells were treated with vehicle or the sulfation inhibitor sodium chlorate, and labelled with either mouse anti-FLAG (a,c) or rabbit anti-FLAG (b,d) antibodies. Images were taken by automated microscopy at 10× magnification. Representative images of three independent experiments; all images taken under equivalent conditions (a,b). Antibody labelling (green), and Hoechst 33258 to stain nuclei (blue); scale bar, 50 μm. The intensity of antibody labelling was quantified, and displayed relative to the HEK 3HA-hCB<sub>2</sub>/FLAG-hD<sub>2</sub> control cell line (c,d). Representative data (mean + SEM) from one of three independent experiments performed in triplicate; all differences between vehicle and sodium chlorate treated cells are statistically significant (\*\*p < 0.01).

distinct signalling phenotype but cannot be demonstrated *in vivo*<sup>42</sup>), and this may be occurring in our experimental system. We also observed that FLAG-hD<sub>2</sub> was more readily detected by both anti-FLAG antibodies in the HEK 3HA-hCB<sub>2</sub> parental cell line than in either of the other experimental cell lines, although all cell lines contained equivalent FLAG-hD<sub>2</sub> expression. This difference in detection was maintained even after inhibition of sulfation, suggesting that the FLAG epitope was more accessible in this cell line in general. This may have occurred through a different pattern of receptor dimerization, altering the accessibility of the FLAG-hD<sub>2</sub> N-terminus for antibodies.

Potentially, the similarity in the effects 3HA-hCB<sub>1</sub> and 3HA-hCB<sub>2</sub> have on FLAG-hD<sub>2</sub> expression are due to altered cell signalling, rather than a direct heterodimerisation interaction. Both CB<sub>1</sub> and CB<sub>2</sub> receptors signal through G $\alpha$ i-pathways, have similar functional effects in cAMP and pERK signalling<sup>43–45</sup>, and are known to exhibit constitutive signalling<sup>46–49</sup>, including in unstimulated HEK cells<sup>19,50</sup>. This constitutive signalling may alter the posttranslational modification repertoire of the cell, thus increasing the frequency of sulfation reactions. While we are not aware of any previous reports of signalling altering sulfation, certainly signalling-mediated changes in post-translational modifications have been reported (for example<sup>51,52</sup>).

We have demonstrated that in the HEK cell line, antibody detectability of the FLAG epitope in the FLAG-hD<sub>2</sub> construct is altered when it is co-expressed with HA-tagged cannabinoid receptors, seemingly via inhibiting posttranslational modification of the FLAG epitope. It is unclear whether this is due to specific physical interactions between D<sub>2</sub> and CB<sub>1</sub>/CB<sub>2</sub>, or an indirect influence of cannabinoid receptors on cellular function which may also affect other GPCRs and proteins. However, sulfation is a fundamental eukaryotic posttranslational modification which could well be influenced by various manipulations or drug treatments. There is therefore considerable potential for FLAG epitope detectability to be influenced unintentionally and this study suggests caution is required when utilising epitope tags, particularly FLAG, for detection of protein expression. Indeed, careful consideration of potential posttranslational modification sites in the target epitope is an important consideration when designing or utilising antibodies in general<sup>53</sup>. In this case our initial hypothesis - that coexpression of CB<sub>1</sub> could stabilise D<sub>2</sub> expression, potentially due to dimerization of the receptors - has transpired to be an artefact of the anti-FLAG antibody labelling that is differentially regulated by cannabinoid receptor expression. Given the widespread use of epitope tags in fundamental receptor studies, this finding has far-reaching consequences for the interpretation of these experiments.

## Materials and Methods

**Plasmid construction.** The FLAG-hD<sub>2</sub> pcDNA3.1+ construct was generated by chimerizing the FLAG epitope to the N-terminus of hD<sub>2</sub> cDNA in pcDNA3.1+ (with the three amino acid linker sequence “EFT” between FLAG and hD<sub>2</sub>, and retaining the start codon of hD<sub>2</sub>; cDNA Resource Centre ([www.cdna.org](http://www.cdna.org)), #DRD0200001). 3HA-hCB<sub>1</sub> pEF4 A and 3HA-hCB<sub>2</sub> pEF4A constructs have been described previously<sup>19,54</sup>.

**Cell culture.** HEK cells were cultured in DMEM with 10% FBS, at 37°C in 5% CO<sub>2</sub>. Stable cell lines expressing 3HA-hCB<sub>1</sub> pEF4A and 3HA-hCB<sub>2</sub> pEF4A constructs were generated by transfection with Lipofectamine 2000 following the manufacturer’s instructions and selected for using 350 µg/ml zeocin. These cells were clonally isolated (HEK 3HA-hCB<sub>1</sub>) or FACS sorted (HEK 3HA-hCB<sub>2</sub>) before use in further experiments.

For stable transfection time course experiments, replicate experiments were performed at least one week apart to ensure that time point observations remained independent. HEK wildtype (wt; ATCC #CRL-1573), HEK 3HA-hCB<sub>1</sub><sup>19</sup> or HEK 3HA-hCB<sub>2</sub><sup>54</sup> cell lines were transfected with FLAG-hD<sub>2</sub> pcDNA3.1+ plasmid, using Lipofectamine 2000 following the manufacturer’s instructions. Two days after transfection, 550 µg/ml G418 was added to the growth media to select for cells harbouring stably-integrated plasmid. Cell lines were passaged twice-weekly, being allowed to get no more than 90% confluent before passaging, and remaining in 550 µg/ml G418 for the duration of the experiment.

**Immunocytochemistry.** Polyclonal anti-FLAG antibody (raised in rabbit) was obtained from Sigma-Aldrich (MO, USA; cat. F7425; lot numbers 001M4789 and 093M4798) and used at a 1:400 or 1:500 dilution respectively, depending on batch. Monoclonal “M2” anti-FLAG antibody (raised in mouse) was also obtained from Sigma-Aldrich (cat. F1804; lot numbers SLBH1191V and 080M6035), and used at approximately 2 µg/ml. Secondary antibodies were obtained from Molecular Probes, Life Technologies (CA, USA): anti-mouse Alexa 488 (cat. A11029), anti-mouse Alexa 594 (cat. A11032), anti-rabbit Alexa 594 (cat. A11037), all raised in goat and used at a 1:400 dilution.

Cells were seeded in poly-L-lysine or poly-D-lysine treated clear 96-well plates, at an appropriate density to ensure 50–80% confluency at the time of antibody application. When required, cells were grown in 50 mM sodium chlorate (in standard growth media) for 48 hours before immunocytochemistry. Primary antibody labelling was performed on live cells, allowing selective labelling of the surface receptor population. Cells were equilibrated with assay media (DMEM + 5 mg/ml BSA) for 30 minutes, then incubated with primary antibodies diluted in assay media for 30 minutes at 37°C to label surface receptors. Cells were then washed twice with assay media before fixation with 50% methanol + 50% acetone at 4°C for 10 minutes. Secondary antibodies were applied after fixation, and diluted in phosphate buffered saline containing 1% normal goat serum, 0.2% Triton X-100, and 0.4 mg/ml thiomersal. Finally, DNA was stained with Hoechst 33258 in phosphate buffered saline containing 0.2% Triton X-100.

Images were acquired using the ImageXpress Micro XLS (Molecular Devices, CA, USA) automated microscope, at 10× magnification, with four sites imaged per well. To analyse the proportion of cells exhibiting antibody labelling above background noise, images were analysed using the MetaXpress (version 5.3.0.4, Molecular Devices) “Multiwavelength cell scoring” function, or the MetaMorph (versions 6 and 10; Molecular Devices)

“Cell scoring” function. These functions identify each cell by nuclear Hoechst staining, followed by segmentation of one or both wavelengths of interest in a user-defined “nucleus and cytoplasm” area.

To analyse the average intensity of labelling across the total population of cells, images were processed using MetaMorph software (versions 6 and 10), using the “Total Grey Value Per Cell” method described by Grimsey, *et al.*<sup>55</sup> with some modifications<sup>56</sup>. This analysis paradigm measures the total intensity of fluorescent antibody labelling above background and averages this intensity of antibody labelling between the total number of nuclei counted per image, thereby providing labelling intensity results as a population average.

**Radioligand binding.** Cells were seeded in poly-D-lysine treated 24-well plates and grown until 50–80% confluent. Cells were then incubated for 30 minutes at 37 °C with assay buffer (DMEM + 5 mg/ml BSA), followed by 30 minutes at 37 °C with [<sup>3</sup>H]-raclopride (Perkin Elmer, MA, USA) at 1.3 nM, with or without 10 μM unlabelled raclopride as a displacer. Assay buffer was removed and cells were washed twice in ice-cold phosphate buffered saline, then lysed in 0.1 M NaOH for 10–20 minutes. Lysate samples were then mixed with scintillation fluid and scintillation events were measured for 3 minutes per sample in a Wallac 1450 MicroBeta TriLux (Perkin Elmer, MA, USA). Lysate samples were also assayed in DC protein assay (Biorad, CA, USA) to enable normalisation to protein concentration.

**cAMP signalling assay.** Cells were transiently transfected using Lipofectamine 2000 with V8-CAMYEL, a bioluminescence resonance energy transfer (BRET)-based cAMP biosensor<sup>57</sup>. 48 hours after transfection, cells were equilibrated with assay buffer (HBSS + 1 mg/ml BSA) for 30 minutes, and then incubated for a further 5 minutes with the luciferase substrate coelenterazine h to a final concentration of 5 μM. Forskolin (an adenylate cyclase agonist) and quinpirole (a selective D<sub>2</sub> agonist) were then added, and luminescence was detected immediately in a VictorXLight plate reader (Perkin Elmer, MA, USA), using 460/25 nm and 535/25 nm filter sets, with temperature control at 37 °C.

An inverse BRET ratio was calculated by dividing the donor signal by the acceptor signal, such that higher BRET ratio reflects greater cytoplasmic cAMP concentration. Inverse BRET ratio responses were measured for 15 minutes, and plotted as a function of time. The overall response over time was determined by an area under the curve calculation, representing the cumulative cAMP response. Data was processed and graphed using Prism (version 6, GraphPad, CA, USA), and agonist responses normalised to Vehicle (0%) and forskolin (100%).

**Data analysis.** Data were plotted and statistical analysis was performed using GraphPad Prism (version 6, GraphPad, CA, USA). The Brown-Forsythe test for equal variance was performed to ensure parametric testing was appropriate. Paired/repeated measures testing was performed in all experimental designs where matching was applicable. Results were analysed with one-way analysis of variance (ANOVA) with Tukey’s multiple comparisons post-hoc testing, or two-way ANOVA with Sidak’s multiple comparisons, as appropriate.

## References

- Venkatakrishnan, A. J. *et al.* Molecular signatures of G-protein-coupled receptors. *Nature* **494**, 185–194 (2013).
- Dupré, D. J., Robitaille, M., Rebois, R. V. & Hébert, T. E. The role of G<sub>βγ</sub> subunits in the organization, assembly, and function of GPCR signaling complexes. *Annu Rev Pharmacol Toxicol* **49**, 31–56 (2009).
- Fuxe, K., Marcellino, D., Guidolin, D., Woods, A. S. & Agnati, L. F. Heterodimers and receptor mosaics of different types of G-protein-coupled receptors. *Physiology (Bethesda, Md)* **23**, 322–332, doi: 10.1152/physiol.00028.2008 (2008).
- Agnati, L. F., Guidolin, D., Vilardaga, J. P., Ciruela, F. & Fuxe, K. On the expanding terminology in the GPCR field: the meaning of receptor mosaics and receptor heteromers. *Journal of receptor and signal transduction research* **30**, 287–303, doi: 10.3109/10799891003786226 (2010).
- Fuxe, K. *et al.* GPCR heteromers and their allosteric receptor-receptor interactions. *Current medicinal chemistry* **19**, 356–363 (2012).
- Pin, J. *et al.* International Union of Basic and Clinical Pharmacology. LXVII. Recommendations for the recognition and nomenclature of G protein-coupled receptor heteromultimers. *Pharmacol Rev* **59**, 5–13 (2007).
- El Khoury, M. A., Gorgievski, V., Moutsimilli, L., Giros, B. & Tzavara, E. T. Interactions between the cannabinoid and dopaminergic systems: evidence from animal studies. *Progress in neuro-psychopharmacology & biological psychiatry* **38**, 36–50, doi: 10.1016/j.pnpbp.2011.12.005 (2012).
- Chiu, C. Q., Puente, N., Grandes, P. & Castillo, P. E. Dopaminergic modulation of endocannabinoid-mediated plasticity at GABAergic synapses in the prefrontal cortex. *The Journal of neuroscience* **30**, 7236–7248 (2010).
- Pickel, V. A., Chan, J., Kearn, C. S. & Mackie, K. Targeting dopamine D<sub>2</sub> and cannabinoid-1 (CB<sub>1</sub>) receptors in rat nucleus accumbens. *J Comp Neurol* **495**, 299–313 (2006).
- Glass, M. & Felder, C. C. Concurrent stimulation of cannabinoid CB<sub>1</sub> and dopamine D<sub>2</sub> receptors augments cAMP accumulation in striatal neurons: evidence for a Gs linkage to the CB<sub>1</sub> receptor. *J Neurosci* **17**, 5327–5333 (1997).
- Kearn, C. S., Blake-Palmer, K., Daniel, E., Mackie, K. & Glass, M. Concurrent stimulation of cannabinoid CB<sub>1</sub> and dopamine D<sub>2</sub> receptors enhances heterodimer formation: a mechanism for receptor cross-talk? *Mol Pharmacol* **67**, 1697–1704 (2005).
- Jarrharian, A., Watts, V. J. & Barker, E. L. D<sub>2</sub> dopamine receptors modulate G<sub>α</sub>-subunit coupling of the CB<sub>1</sub> cannabinoid receptor. *J Pharmacol Exp Ther* **308**, 880–886 (2004).
- Khan, S. S. & Lee, F. J. S. Delineation of Domains Within the Cannabinoid CB<sub>1</sub> and Dopamine D<sub>2</sub> Receptors That Mediate the Formation of the Heterodimer Complex. *Journal of Molecular Neuroscience* **53**, 10–21 (2014).
- Marcellino, D. *et al.* Antagonistic cannabinoid CB<sub>1</sub>/dopamine D<sub>2</sub> receptor interactions in striatal CB<sub>1</sub>/D<sub>2</sub> heteromers. A combined neurochemical and behavioral analysis. *Neuropharmacol* **54**, 815–823 (2008).
- Carriba, P. *et al.* Detection of heteromerization of more than two proteins by sequential BRET-FRET. *Nature Methods* **5**, 727–733 (2008).
- Navarro, G. *et al.* Interactions between intracellular domains as key determinants of the quaternary structure and function of receptor heteromers. *J Biol Chem* **285**, 27346–27359 (2010).
- Przybyla, J. A. & Watts, V. J. Ligand-induced regulation and localization of cannabinoid CB<sub>1</sub> and dopamine D<sub>2</sub>L receptor heterodimers. *J Pharmacol Exp Ther* **332**, 710–719 (2010).
- Blume, L. C. *et al.* Striatal CB<sub>1</sub> and D<sub>2</sub> receptors regulate expression of each other, CRIP1A and delta opioid systems. *Journal of neurochemistry* **124**, 808–820 (2013).
- Cawston, E. E. *et al.* Real-time characterization of cannabinoid receptor 1 (CB<sub>1</sub>) allosteric modulators reveals novel mechanism of action. *British Journal of Pharmacology* **170**, 893–907, doi: 10.1111/bph.12329 (2013).



20. Choe, H. & Farzan, M. In *Methods in Enzymology* Vol. Volume 461 (eds M. Handel Tracy & J. Hamel Damon) 147–170 (Academic Press, 2009).
21. Schmidt, P. M. *et al.* Taking down the FLAG! How Insect Cell Expression Challenges an Established Tag-System. *PLoS ONE* **7**, e37779, doi: 10.1371/journal.pone.0037779 (2012).
22. Tan, J. H. Y. *et al.* Tyrosine Sulfation of Chemokine Receptor CCR2 Enhances Interactions with Both Monomeric and Dimeric Forms of the Chemokine Monocyte Chemoattractant Protein-1 (MCP-1). *Journal of Biological Chemistry* **288**, 10024–10034, doi: 10.1074/jbc.M112.447359 (2013).
23. Michel, M. C., Wieland, T. & Tsujimoto, G. How reliable are G-protein-coupled receptor antibodies? *Naunyn-Schmiedeberg's archives of pharmacology* **379**, 385–388 (2009).
24. Marchalant, Y., Brownjohn, P. W., Bonnet, A., Kleffmann, T. & Ashton, J. C. Validating Antibodies to the Cannabinoid CB2 Receptor: Antibody Sensitivity Is Not Evidence of Antibody Specificity. *Journal of Histochemistry & Cytochemistry* **62**, 395–404, doi: 10.1369/0022155414530995 (2014).
25. Baek, J.-H., Darlington, C. L., Smith, P. F. & Ashton, J. C. Antibody testing for brain immunohistochemistry: Brain immunolabeling for the cannabinoid CB2 receptor. *Journal of Neuroscience Methods* **216**, 87–95, doi: http://dx.doi.org/10.1016/j.jneumeth.2013.03.021 (2013).
26. Grimsey, N. L. *et al.* Specific detection of CB1 receptors; cannabinoid CB1 receptor antibodies are not all created equal! *J Neurosci Methods* **171**, 78–86, doi: 10.1016/j.jneumeth.2008.02.014 (2008).
27. Koenig, J. A. Assessment of receptor internalization and recycling. *Methods in molecular biology* **259**, 249–273, doi: 10.1385/1-59259-754-8:249 (2004).
28. Salahpour, A. & Barak, L. S. Visualizing receptor endocytosis and trafficking. *Methods Mol Biol.* **756**, 311–23. doi: 10.1007/978-1-61779-160-4\_18 (2011).
29. Lee, R. W. & Huttner, W. B. Tyrosine-O-sulfated proteins of PC12 pheochromocytoma cells and their sulfation by a tyrosylprotein sulfotransferase. *J Biol Chem* **258**, 11326–11334 (1983).
30. Yang, Y.-S. *et al.* Tyrosine Sulfation as a Protein Post-Translational Modification. *Molecules* **20**, 2138 (2015).
31. Monigatti, F., Hekking, B. & Steen, H. Protein sulfation analysis—A primer. *Biochimica et Biophysica Acta (BBA) - Proteins and Proteomics* **1764**, 1904–1913, doi: http://dx.doi.org/10.1016/j.bbapap.2006.07.002 (2006).
32. Fieger, C. B., Huang, M.-C., Van Brocklyn, J. R. & Goetzl, E. J. Type 1 sphingosine 1-phosphate G protein-coupled receptor signaling of lymphocyte functions requires sulfation of its extracellular amino-terminal tyrosines. *The FASEB journal : official publication of the Federation of American Societies for Experimental Biology* **19**, 1926–1928, doi: 10.1096/fj.05-4476fj (2005).
33. Liu, Z.-j. *et al.* Tyrosine sulfation in N-terminal domain of human C5a receptor is necessary for binding of chemotaxis inhibitory protein of *Staphylococcus aureus*. *Acta Pharmacol Sin* **32**, 1038–1044 (2011).
34. Baeuerle, P. A. & Huttner, W. B. Chlorate—a potent inhibitor of protein sulfation in intact cells. *Biochemical and biophysical research communications* **141**, 870–877 (1986).
35. Mintz, K. P., Fisher, L. W., Grzesik, W. J., Hascall, V. C. & Midura, R. J. Chlorate-induced inhibition of tyrosine sulfation on bone sialoprotein synthesized by a rat osteoblast-like cell line (UMR 106-01 BSP). *Journal of Biological Chemistry* **269**, 4845–4852 (1994).
36. Pouyani, T. & Seed, B. PSGL-1 recognition of P-selectin is controlled by a tyrosine sulfation consensus at the PSGL-1 amino terminus. *Cell* **83**, 333–343 (1995).
37. Ji, Y. *et al.* Role of dysbindin in dopamine receptor trafficking and cortical GABA function. *Proceedings of the National Academy of Sciences* **106**, 19593–19598, doi: 10.1073/pnas.0904289106 (2009).
38. Namkung, Y. & Sibley, D. R. Protein Kinase C Mediates Phosphorylation, Desensitization, and Trafficking of the D2 Dopamine Receptor. *Journal of Biological Chemistry* **279**, 49533–49541, doi: 10.1074/jbc.M408319200 (2004).
39. Oceau, J. C. *et al.* G Protein Beta 5 Is Targeted to D2-Dopamine Receptor-Containing Biochemical Compartments and Blocks Dopamine-Dependent Receptor Internalization. *PLoS one* **9**, e105791 (2014).
40. Sharma, M., Cerver, J., Oceau, J. C. & Koo, A. Plasma Membrane Compartmentalization of D2 Dopamine Receptors. *Journal of Biological Chemistry* **288**, 12554–12568, doi: 10.1074/jbc.M112.443945 (2013).
41. Kabbani, N., Negyessy, L., Lin, R., Goldman-Rakic, P. & Levenson, R. Interaction with Neuronal Calcium Sensor NCS-1 Mediates Desensitization of the D2 Dopamine Receptor. *The Journal of Neuroscience* **22**, 8476–8486 (2002).
42. Frederick, A. *et al.* Evidence against dopamine D1/D2 receptor heteromers. *Molecular Psychiatry* **20**(11), 1373–85. doi: 10.1038/mp.2014.166 (2015).
43. Bouaboula, M. *et al.* Signaling Pathway Associated with Stimulation of CB2 Peripheral Cannabinoid Receptor. *European Journal of Biochemistry* **237**, 704–711, doi: 10.1111/j.1432-1033.1996.0704p.x (1996).
44. Galve-Roperh, I., Rueda, D., Gómez del Pulgar, T., Velasco, G. & Guzmán, M. Mechanism of Extracellular Signal-Regulated Kinase Activation by the CB1 Cannabinoid Receptor. *Molecular Pharmacology* **62**, 1385–1392, doi: 10.1124/mol.62.6.1385 (2002).
45. Pertwee, R. G. *et al.* International Union of Basic and Clinical Pharmacology. LXXIX. Cannabinoid receptors and their ligands: beyond CB1 and CB2. *Pharmacological reviews* **62**, 588–631 (2010).
46. Bouaboula, M. *et al.* A selective inverse agonist for central cannabinoid receptor inhibits mitogen-activated protein kinase activation stimulated by insulin or insulin-like growth factor 1. Evidence for a new model of receptor/ligand interactions. *J Biol Chem* **272**, 22330–22339 (1997).
47. Landsman, R. S., Burkey, T. H., Consroe, P., Roeske, W. R. & Yamamura, H. I. SR141716A is an inverse agonist at the human cannabinoid CB1 receptor. *Eur J Pharmacol* **334**, R1–2 (1997).
48. MacLennan, S. J., Reynen, P. H., Kwan, J. & Bonhaus, D. W. Evidence for inverse agonism of SR141716A at human recombinant cannabinoid CB1 and CB2 receptors. *Br J Pharmacol* **124**, 619–622, doi: 10.1038/sj.bjp.0701915 (1998).
49. Glass, M. & Northup, J. K. Agonist Selective Regulation of G Proteins by Cannabinoid CB1 and CB2 Receptors. *Molecular Pharmacology* **56**, 1362–1369, doi: 10.1124/mol.56.6.1362 (1999).
50. Canals, M. & Milligan, G. Constitutive activity of the cannabinoid CB1 receptor regulates the function of co-expressed Mu opioid receptors. *Journal of Biological Chemistry* **283**, 11424–11434 (2008).
51. Zhang, P., Fu, W. Y., Fu, A. K. & Ip, N. Y. S-nitrosylation-dependent proteasomal degradation restrains Cdk5 activity to regulate hippocampal synaptic strength. *Nature communications* **6**, 8665, doi: 10.1038/ncomms9665 (2015).
52. Dodson, M., Redmann, M., Rajasekaran, N. S., Darley-Usmar, V. & Zhang, J. KEAP1-NRF2 signalling and autophagy in protection against oxidative and reductive proteotoxicity. *The Biochemical journal* **469**, 347–355, doi: 10.1042/bj20150568 (2015).
53. Hancock, D. C., O' Reilly, N. J. & Evan, G. I. Synthesis of peptides for use as immunogens. *Immunochemical Protocols*. 69–79, doi: 10.1007/978-1-59259-257-9\_7 (1998).
54. Grimsey, N. L., Goodfellow, C. E., Dragunow, M. & Glass, M. Cannabinoid receptor 2 undergoes Rab5-mediated internalization and recycles via a Rab11-dependent pathway. *Biochimica et Biophysica Acta (BBA) - Molecular Cell Research* **1813**, 1554–1560, doi: http://dx.doi.org/10.1016/j.bbamcr.2011.05.010 (2011).
55. Grimsey, N. L., Narayan, P. J., Dragunow, M. & Glass, M. A novel high-throughput assay for the quantitative assessment of receptor trafficking. *Clinical and Experimental Pharmacology and Physiology* **35**, 1377–1382, doi: 10.1111/j.1440-1681.2008.04991.x (2008).
56. Finlay, D. B., Joseph, W. R., Grimsey, N. L. & Glass, M. GPR18 undergoes a high degree of constitutive trafficking but is unresponsive to N-Arachidonoyl Glycine. *PeerJ* **4**, e1835 (2016).
57. Hunter, M. R., Edgar, S. G., Finlay, D. B. & Glass, M. In *Australasian Society of Clinical and Experimental Pharmacologists and Toxicologists (ASCEPT) and the Molecular Pharmacology of GPCRs (MP-GPCR) 2014 Joint Scientific Meeting* (Melbourne, Australia, 2014).

## Acknowledgements

This work was funded by a grant from the Royal Society of New Zealand Marsden Fund.

## Author Contributions

M.R.H. designed and performed experiments, wrote manuscript. N.L.G. designed experiments and analysis, wrote manuscript. M.G. designed experiments, wrote manuscript.

## Additional Information

**Competing financial interests:** The authors declare no competing financial interests.

**How to cite this article:** Hunter, M. R. *et al.* Sulfation of the FLAG epitope is affected by co-expression of G protein-coupled receptors in a mammalian cell model. *Sci. Rep.* **6**, 27316; doi: 10.1038/srep27316 (2016).



This work is licensed under a Creative Commons Attribution 4.0 International License. The images or other third party material in this article are included in the article's Creative Commons license, unless indicated otherwise in the credit line; if the material is not included under the Creative Commons license, users will need to obtain permission from the license holder to reproduce the material. To view a copy of this license, visit <http://creativecommons.org/licenses/by/4.0/>